Macrophage- and CD4+ T cell-derived SIV differ in glycosylation, infectivity and neutralization sensitivity

Christina B. Karsten, Falk F. R. Büttner, Samanta Cajic, Inga Nehlmeier, Berit Roshani, Antonina Klippert, Ulrike Sauermann, Nicole Stolte-Leeb, Udo Reichl, Rita Gerardy-Schahn, Erdmann Rapp, Christiane Stahl-Hennig, Stefan Pöhlmann
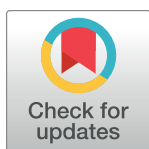
PLOS PATHOGENS

Macrophage- and CD4+ T cell-derived SIV differ in glycosylation, infectivity and neutralization sensitivity

Christina B. Karsten[1]*, Falk F. R. Buettner[2,3©], Samanta Cajic[4,5©], Inga Nehlmeier[6], Berit Roshani[7], Antonina Klippert[8], Ulrike Sauermann[7], Nicole Stolte-Leeb[7], Udo Reichl[5], Rita Gerardy-Schahn[2], Erdmann Rapp[4,5], Christiane Stahl-Hennig[7], Stefan Pöhlmann[6,9]*

1 Institute for the Research on HIV and AIDS-associated Diseases, University Hospital Essen, University of Duisburg-Essen, Essen, Germany, 2 Institute of Clinical Biochemistry, Hannover Medical School, Hannover, Germany, 3 Proteomics, Institute of Theoretical Medicine, Faculty of Medicine, University of Augsburg, Augsburg, Germany, 4 glyXera GmbH, Magdeburg, Germany, 5 Bioprocess Engineering Group, Max Planck Institute for Dynamics of Complex Technical Systems, Magdeburg, Germany, 6 Infection Biology Unit, German Primate Center–Leibniz Institute for Primate Research, Göttingen, Germany, 7 Unit of Infection Models, German Primate Center–Leibniz Institute for Primate Research, Göttingen, Germany, 8 Nuvisan ICB GmbH, Berlin, Germany, 9 Faculty of Biology and Psychology, Georg-August-University Göttingen, Göttingen, Germany

© These authors contributed equally to this work.
* christina.karsten@uni-due.de (CBK); spoehlmann@dpz.eu (SP)

Abstract

The human immunodeficiency virus (HIV) envelope protein (Env) mediates viral entry into host cells and is the primary target for the humoral immune response. Env is extensively glycosylated, and these glycans shield underlying epitopes from neutralizing antibodies. The glycosylation of Env is influenced by the type of host cell in which the virus is produced. Thus, HIV is distinctly glycosylated by CD4+ T cells, the major target cells, and macrophages. However, the specific differences in glycosylation between viruses produced in these cell types have not been explored at the molecular level. Moreover, it remains unclear whether the production of HIV in CD4+ T cells or macrophages affects the efficiency of viral spread and resistance to neutralization. To address these questions, we employed the simian immunodeficiency virus (SIV) model. Glycan analysis implied higher relative levels of oligomannose-type N-glycans in SIV from CD4+ T cells (T-SIV) compared to SIV from macrophages (M-SIV), and the complex-type N-glycans profiles seem to differ between the two viruses. Notably, M-SIV demonstrated greater infectivity than T-SIV, even when accounting for Env incorporation, suggesting that host cell-dependent factors influence infectivity. Further, M-SIV was more efficiently disseminated by HIV binding cellular lectins. We also evaluated the influence of cell type-dependent differences on SIV's vulnerability to carbohydrate binding agents (CBAs) and neutralizing antibodies. T-SIV demonstrated greater susceptibility to mannose-specific CBAs, possibly due to its elevated expression of oligomannose-type N-glycans. In contrast, M-SIV exhibited higher susceptibility to neutralizing sera in comparison to T-SIV. These findings underscore the importance of host cell-

dependent attributes of SIV, such as glycosylation, in shaping both infectivity and the potential effectiveness of intervention strategies.

Author summary

The human immunodeficiency virus (HIV) is the causative agent of the acquired immunodeficiency syndrome (AIDS), a lethal condition that necessitates life-long antiretroviral therapy for prevention. The envelope protein (Env) of HIV mediates the viral entry into host cells and is the sole target for the immune system on the surface of the virus. Env's extensive modification with sugars, so called N-glycans, shields crucial epitopes from neutralizing antibodies. Interestingly, key HIV producing cell types, such as CD4⁺ T cells and macrophages, modify Env with distinct N-glycosylation patterns. However, the specific molecular disparities in N-glycosylation between viruses from these cell types are unexplored, and whether the producer cell type impacts the viral spread and resistance to neutralization is incompletely understood.

Utilizing the simian immunodeficiency virus (SIV) as a model for HIV, our study revealed differing N-glycan profiles between SIV Env produced in CD4⁺ T cells (T-SIV) and macrophages (M-SIV), with T-SIV incorporating more N-glycans of the oligomannose-type into Env than M-SIV. M-SIV displayed enhanced infectivity and transmissibility in *in vitro* studies. Additionally, M-SIV exhibited greater susceptibility to neutralizing sera compared to T-SIV, while T-SIV showed heightened susceptibility to mannose-specific carbohydrate-binding agents. These findings emphasize the critical role of host cell-dependent attributes in shaping N-glycosylation of Env as well as viral infectivity and spread. These findings have important implications for the development of new biomedical interventions against HIV.

Introduction

More than four decades since its discovery, the human immunodeficiency virus (HIV) and the associated disease, acquired immunodeficiency syndrome (AIDS), remain a significant global health challenge. In 2021, UNAIDS reported that 1.3 million individuals contracted HIV, and 630,000 AIDS-related deaths were observed [1]. To combat this ongoing crisis, the development of vaccines and innovative antiviral strategies is crucial. The success of these initiatives will be based on a profound understanding of the complex interplay between HIV and its primary host cells, CD4⁺ T cells and macrophages.

The viral envelope protein, Env, mediates entry of HIV into host cells and constitutes the sole target for neutralizing antibodies [2]. Env is synthesized as an inactive precursor protein, gp160, in the secretory pathway of infected cells. During its trafficking through the Golgi apparatus, gp160 is proteolytically cleaved by furin into the surface unit, gp120, and the transmembrane unit, gp41 [3], which remain non-covalently associated. For host cell entry, gp120 binds to the CD4 receptor and a chemokine coreceptor, usually C-C motif chemokine receptor 5 (CCR5) and/or C-X-C motif chemokine receptor 4 (CXCR4). Binding to receptor and coreceptor activates gp41, which drives the fusion of the viral and the target cell membranes, enabling the delivery of the viral genetic information into the host cell cytoplasm [4].

A hallmark of Env, a trimeric type I transmembrane protein, is its extensive glycosylation, particularly of gp120, accounting for roughly 50% of the molecular mass [5]. The glycans play

a key role in viral spread: they shield underlying epitopes from attack by neutralizing antibodies [6] and facilitate viral capture by immune cell lectins like dendritic cell-specific intercellular adhesion molecule-grabbing nonintegrin (DC-SIGN) [7], which likely play an important role in mucosal transmission. The fundamental importance of the glycan shield is underscored by its adaptation in response to the humoral immune response [6], and disrupting N-glycosylation signals of Env can render HIV [8–10] and the closely related simian immunodeficiency virus (SIV) susceptible to neutralization [11,12].

The process of N-glycosylation involves the transfer of a preformed oligosaccharide precursor linked to dolichol-phosphate (Dol-P-P-GlcNAc$_2$Man$_9$Glc$_3$) onto asparagine residues within the consensus sequon Asn-X-Ser/Thr of nascent Env by the ER-localized oligosaccharyltransferase [13]. Following precursor attachment, initial trimming steps carried out by highly conserved ER resident glycosidases occur, which together with the action of glycosyltransferase, play pivotal roles in the regulation of Env folding and transport [13]. Only the fully folded trimeric Env enters the Golgi apparatus, where oligomannose-type glycans, generated in the ER, undergo further trimming and extension into hybrid and complex forms, potentially containing fucose, galactose, N-acetylglucosamine (GlcNAc), sialic acids (e.g. N-acetylneuraminic acid, N-glycolylneuraminic acid) [13], and structures like N-acetylgalactosamine (GalNAc)β1–4GlcNAc (LacdiNAc) (Fig 1A). However, the level of N-glycan processing depends on the quaternary structure of Env and more than half of the N-glycans are not fully accessible to enzymatic processing due to their recessed location or to extremely dense glycan packaging, and thus remain in the oligomannose-type state [5,14].

Glycosylation of Env and cellular proteins is a cell type-dependent process [15–18] and differences in N-glycosylation of the viral Env protein have been observed upon production of HIV and SIV in the viral target cells, CD4+ T cells and macrophages [15,19]. Further, viruses from macrophages and T cells seemed to differ in infectivity [19, 20], neutralization sensitivity [15,20] and lectin reactivity [20,21]. Despite their importance in virus-host cell interactions and immune control, host cell-specific glycosylation differences have not been determined for HIV or SIV at a molecular level. Furthermore, a detailed comparative analysis of the biological properties of isogenic HIV and SIV produced in macrophages and CD4+ T cells has been lacking. In this study, we aim to address these knowledge gaps by strategically investigating the influence of macrophage or CD4+ T cell origin on the significance of Env glycosylation, viral spread, and neutralization sensitivity, using SIV as a model for HIV.

Results

Production of SIV in macrophages and CD4+ T cells

To produce isogenic SIV in CD4+ T cells and macrophages, it was imperative to employ a molecularly cloned SIV variant capable of robust replication in both cell types. Our choice for this purpose was a SIVmac239 variant, specifically SIVmac239/316 Env, characterized by nine amino acid substitutions within Env in comparison to the parental strain [22,23]. These substitutions facilitate efficient utilization of CCR5 in the absence of or at very low levels of CD4 expression [24], a condition observed in rhesus macaque macrophages [25]. For the preparation of SIVmac239/316 Env stocks, CD4+ T cells and macrophages were generated from rhesus macaque peripheral blood mononuclear cells (PBMCs) and their identity was confirmed by analysis of cell surface marker expression via flow cytometry (S1 Fig). Subsequently, CD4+ T cell and macrophage cultures were infected with SIVmac239/316 Env, input virus was removed, and the culture supernatants harvested over a two-week period. Supernatants containing more than 10 ng p27/ml were pooled to generate SIV stocks from macrophages (M-SIV) or CD4+ T cells (T-SIV). The resulting M-SIV and T-SIV stocks featured a
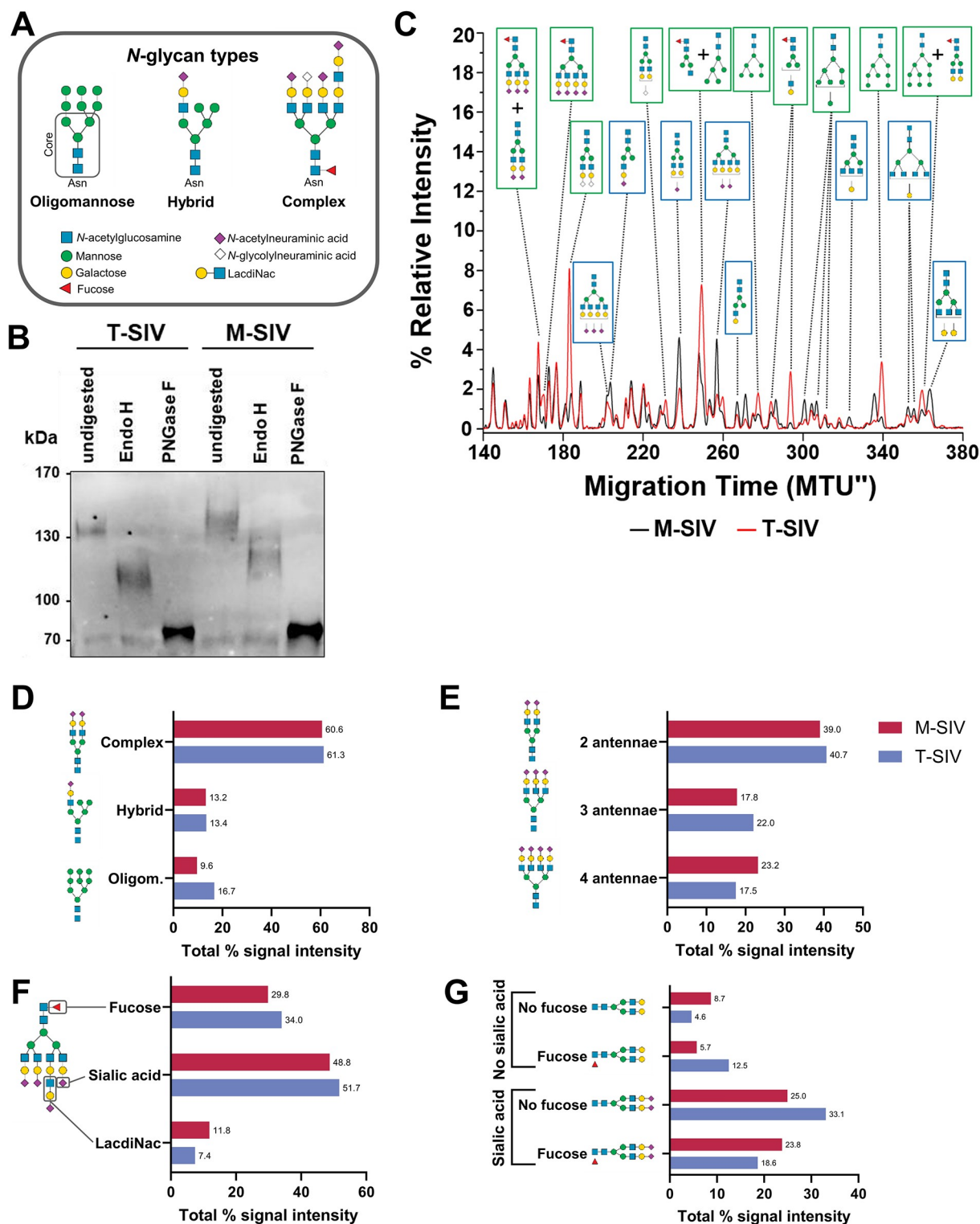
Fig 1. CD4+ T cell-derived simian immunodeficiency virus (T-SIV) gp120 carries more oligomannose-type glycans than gp120 of macrophage-derived SIV (M-SIV). A) Depiction of the different types of N-linked glycans and legend for the glycan moieties shown in Figs 1 and S2. Each N-glycan core consisting of two N-acetylglucosamine and three mannose residues is anchored to the asparagine of an N-linked glycan binding site. The core's mannose residues are directly extended by either exclusively mannose (oligomannose-type), only glycan moieties that are not mannose (complex-type), or a mixture of both (hybrid-type). B) T-SIV and M-SIV viral stocks were normalized for comparable gp120 content and concentrated. The viruses were subjected to mock treatment or enzymatic digestion with endoglycosidase H

(Endo H) or peptide-*N*-glycosidase F (PNGase F), followed by western blot detection of the envelope protein (Env). Consistent results were obtained across three independent experiments. C-G) Differences in the relative distribution of *N*-glycans from gp120 of M-SIV and T-SIV were determined by multiplexed capillary gel electrophoresis with laser-induced fluorescence detection (xCGE-LIF). C) The electropherogram region with the most striking differences between M-SIV and T-SIV is plotted (140–380 migration time units (MTU")). Peak intensities are presented as percentage of the total peak height to obtain the relative signal intensity (in %) for each peak (representing at least one *N*-glycan structure). A selection of distinct *N*-glycan structures enriched in T-SIV are denoted with green boxes, while those enriched in M-SIV are marked with blue boxes. D-G) To delve deeper into the distinctions in the *N*-linked glycan profile of M-SIV and T-SIV gp120, we aggregated the xCGE-LIF signal intensities of peaks corresponding to glycan species associated with specific groups to calculate the total % signal intensity. These data were calculated based on the information provided in S2 Fig. D) illustrates the distribution of annotated glycan species across various glycan types, while E-G) categorizes complex glycans based on their distinct features. Numbers at the end of bars give the exact total % signal intensity for the specific glycan group. Oligom. = oligomannose. Symbolic representation of *N*-glycan structures in the figure were drawn with the software GlycanBuilder2 [61]: green circle, mannose; yellow circle, galactose; blue square, *N*-acetylglucosamine; diamonds, sialic acid (pink: *N*-acetylneuraminic acid, white: *N*-glycolylneuraminic acid); red triangle, fucose.

p27-concentration of 7.9 and 52.2 ng/ml, RNA genome copies of 2.98×10^7 and 2.13×10^8/ml, and a $TCID_{50}$ of 80.353 and 28.184, respectively. Finally, sequencing of *env*, which was amplified through reverse transcriptase-polymerase chain reaction (RT-PCR) from the culture supernatants, provided confirmation that no genetic mutations were introduced into M-SIV or T-SIV throughout the *in vitro* propagation process.

The quantity of oligomannose-type and certain complex *N*-glycans of gp120 differs between M-SIV and T-SIV

The glycan shield of both HIV and SIV plays a pivotal role in immune evasion and mediating lectin-dependent interactions with immune cells. It is plausible that these functions could be modulated by cell type-specific alterations in the glycosylation pattern. To determine whether M-SIV and T-SIV differed in the *N*-glycosylation of the viral Env protein, we subjected concentrated virions to enzymatic digestion using endoglycosidase H (Endo H), which selectively removes oligomannose-type and certain hybrid-type *N*-glycans, and peptide-*N*-glycosidase F (PNGase F), which eliminates all *N*-linked glycans. The band shift upon Endo H digestion was more pronounced for T-SIV than M-SIV suggesting that T-SIV gp120 is adorned with a higher proportion of oligomannose-type glycans compared to M-SIV gp120 (Fig 1B). These findings align with previously published data [15,19,21] but do not offer insights into the specific structures of the differentially incorporated *N*-glycan species.

To address the latter question, we performed *N*-glycan analytics of T-SIV and M-SIV gp120 by multiplexed capillary gel electrophoresis with laser-induced fluorescence detection (xCGE-LIF). Further, the identity of the proteins subjected to *N*-glycan analytics was confirmed by liquid chromatography-tandem mass spectrometry (LC-MS/MS). The xCGE-LIF fingerprints of *N*-glycans derived from M-SIV and T-SIV gp120 show considerable differences in the relative intensities of the detected peaks suggesting quantitative differences in the incorporated glycan species (Figs 1C and S2).

A relative quantification of *N*-glycan signal intensities was performed. For this, the total peak intensity (tpi) of a peak was allocated to all *N*-glycan groups of the analysis, for which the assigned single or multiple glycan species met the criteria. This analysis revealed the following: T-SIV exhibited increased relative levels of oligomannose structures on gp120 compared to M-SIV (Fig 1D, 16.7% vs. 9.6% of tpi); in alignment with the results from glycosidase digestion and subsequent western blot analysis (Fig 1B). Additionally, profiles of complex-type *N*-glycans differed between the two viruses (Fig 1E–1G). M-SIV gp120 displayed more extensive branching of complex glycans, with a higher proportion featuring four antennae rather than three, in comparison to T-SIV (23.2% vs. 17.5% tpi) (Fig 1E). An overall assessment of fucose, sialic acid, and LacdiNAc content revealed that T-SIV gp120 harbors increased levels of *N*-

glycan species carrying fucose (34 vs. 29.8 tpi) and sialic acid (51.7 vs. 48.8 tpi) compared to M-SIV; while the latter exhibited more LacdiNAc (11.8 vs. 7.4 tpi) containing structures (Fig 1F). A more detailed analysis of the complex-type glycan species revealed a more nuanced pattern: M-SIV complex glycans tended to feature either both fucose and sialic acid residues (23.8 (M-SIV) vs. 18.6% tpi (T-SIV)) or neither (8.7 (M-SIV) vs. 4.6% tpi (T-SIV)). Differently, T-SIV complex glycans tended to have either fucose (12.5 (T-SIV) vs. 5.7% tpi (M-SIV)) or sialic acid (33.1 (T-SIV) vs. 25% tpi (M-SIV)) but not both (Fig 1G). Our study revealed for the first time that despite an overall similar N-glycome, M-SIV and T-SIV gp120 differ in their oligomannose-type N-glycan content and complex N-glycan profiles, although due the use of a single pooled virus stock for M-SIV and T-SIV throughout the whole study our analysis was insufficiently powered to determine whether these differences were statistically significant.

M-SIV is better equipped for both direct and indirect viral spread compared to T-SIV

The revelation that M-SIV and T-SIV exhibit disparities in glycan coat composition raised the question of whether the differential origin of M-SIV and T-SIV is also linked to variations in other SIV characteristics pertinent to viral dissemination. To investigate this possibility, our initial focus was on viral infectivity. When TZM-bl indicator cells were exposed to viruses normalized for p27-capsid content, it became evident that M-SIV exhibited significantly higher infectivity than T-SIV (Fig 2A, left panel, 2-way ANOVA, p = 0.03). However, both viruses exhibited *in vivo* infectivity and replicated to comparable levels (S3 Fig), and when we equalized for the infectivity of M-SIV and T-SIV stocks, the infection efficiency on TZM-bl cells was found to be similar (Fig 2A, right panel). These results underscore that the infectivity of M-SIV per ng capsid antigen surpasses that of T-SIV, confirming the findings previously obtained for SIV [19] and dual-tropic HIV [20].

Glycosylation also affects HIV Env incorporation into viral particles [26]. To clarify whether the increased M-SIV infectivity in comparison to T-SIV could be attributed solely to disparities in Env incorporation, we subjected p27-capsid normalized quantities of both M-SIV and T-SIV to western blot analysis to assess their gp120 and p27 content, and quantified the signal using the software ImageJ (Fig 2B and 2C). A visual examination already revealed that the less infectious T-SIV exhibited lower levels of gp120 incorporation compared to the more infectious M-SIV (Fig 2B). Following quantification and subsequent normalization of the gp120 signal to the p27-capsid signal, the data indicated a noteworthy 62% reduction in Env incorporation for T-SIV when compared to M-SIV (Fig 2C, t-test, p = 0.0051). While this effect is significant, the disparities in infectivity between the two viruses (Fig 2A, left panel, 55-fold at 6 ng p27/ml) surpasses the differences in Env incorporation. More research is needed to confirm a linear relationship between Env incorporation and SIV infectivity, however, these data imply a broader impact of the virus-producing cell on SIV infectivity beyond its influence on Env incorporation.

Lectins modulate HIV and SIV transmission to susceptible cells *in vitro* [7,27–29], a process possibly relevant for early viral spread after transmission *in vivo* [30]. Since both M-SIV and T-SIV were found to be infectious in rhesus macaques via the rectal route (S3 Fig), the question arose whether the cell type-dependent differences in these viruses influence their engagement of lectin receptors. Specifically, the interactions of M-SIV and T-SIV with the lectins with potential positive (DC-SIGN [7], DC-SIGN related protein (DC-SIGNR) [29]) or negative (Langerin [28]) influence on HIV/SIV viral spread were investigated. For this purpose a previously published transmission assay was employed [31]. CEMx174 R5 target cells were infected in two ways: directly with either virus, normalized for equal infectivity, or indirectly
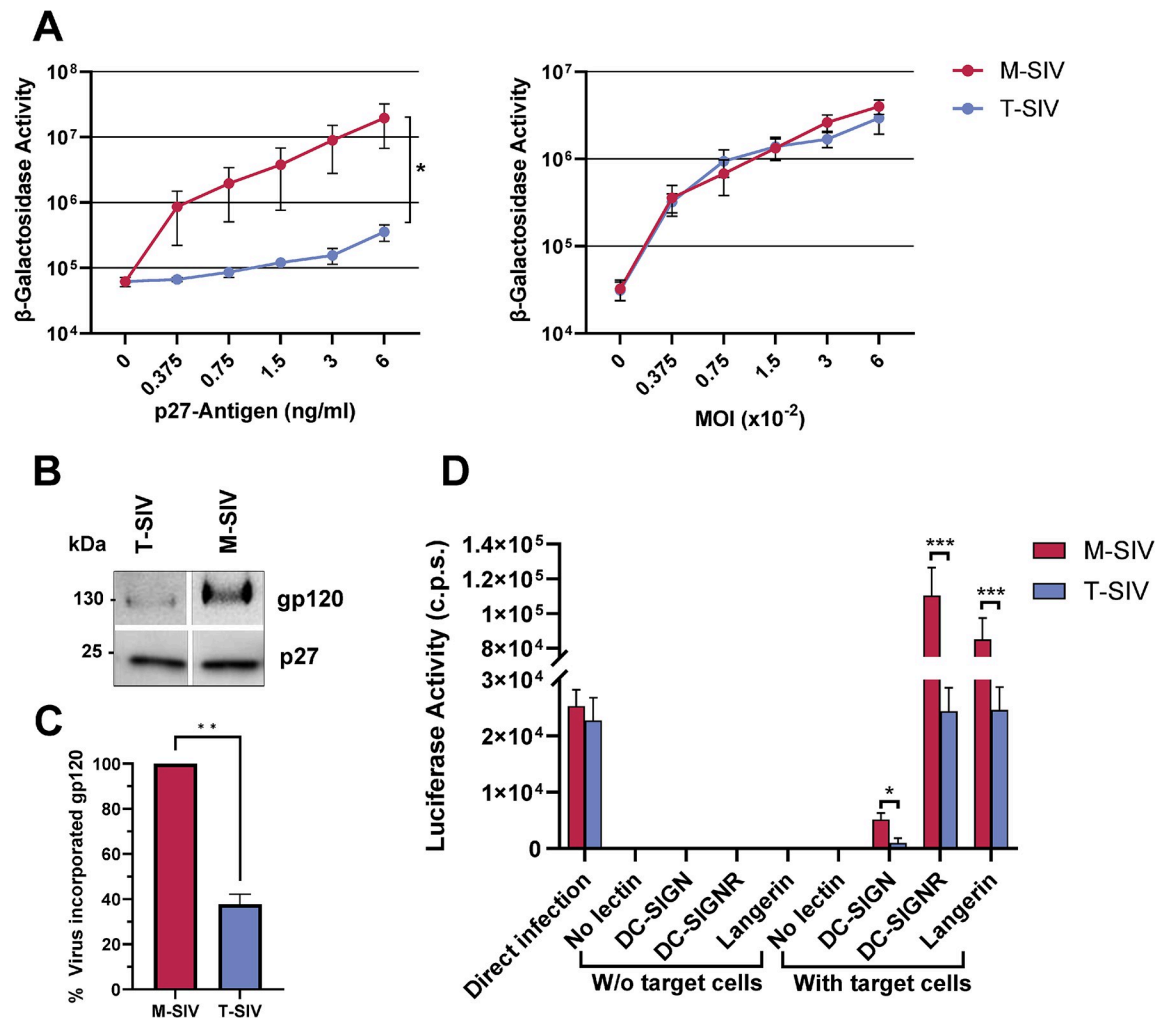
Fig 2. M-SIV is more infectious and better transmitted by cellular lectins than T-SIV. A) TZBM-bl indicator cells were exposed to equal volumes of M-SIV and T-SIV stocks, normalized for p27-capsid protein (left panel) or infectious units (right panel). Following virus removal at 5–6 hours post-infection, β-galactosidase activity was measured in cell lysates 72 hours post-infection. The grand mean of three experiments performed in triplicates (left panel) or quadruplicates (right panel) are shown with the standard error of the mean (SEM). Statistical significance between datasets determined by two-way ANOVA (*, $p \leq 0.05$). B-C) B) M-SIV and T-SIV normalized for equal amounts of p27 were concentrated, resolved using SDS-PAGE, and analyzed by western blot for gp120 and p27. Consistent outcomes were observed across three independent experiments. C) The software ImageJ [55] was utilized to quantify gp120 and p27 signal intensities obtained in B). The gp120 signal per p27 signal ratio was calculated, and values were plotted, with M-SIV set as 100%. Presented is the grand mean with SEM. Paired t-test was applied to assess statistical differences between groups (**, $p \leq 0.01$). D) M-SIV and T-SIV normalized for comparable infectivity on CEMx173 R5 target cells were incubated with Raji cells expressing no additional lectin, dendritic cell-specific intercellular adhesion molecule-grabbing nonintegrin (DC-SIGN), DC-SIGN related protein (DC-SIGNR) or Langerin. Unbound virus was removed and the transmitter cells were co-cultured with CEMx174 R5 target cells. Infection of target cells was detected by the measurement of luciferase activity in cell lysates 72 h post infection. Direct infection of CEMx174 R5 cells served as positive control, while negative controls consisted of Raji cells incubated without target cells. The signals obtained for the transinfection using transmitter cells expressing no lectin were subtracted as background signal. The grand mean of three independent experiments conducted in triplicates with SEM is depicted. Statistical differences between M-SIV and T-SIV for each transmitting lectin were calculated by t-test (*, $p < = 0.05$; ***, $p < = 0.001$). C.p.s.: counts per second.

https://doi.org/10.1371/journal.ppat.1012190.g002

via co-culture with Raji transmitter cells bearing either no lectin or the aforementioned lectins (Fig 2D). While direct infection of target cells confirmed the equivalent infectivity of M-SIV and T-SIV, and co-culturing the virus with transmitter cells in the absence of target cells yielded only background signals, a significant difference emerged. M-SIV was more efficiently

transferred to target cells by DC-SIGN compared to T-SIV (t-test, p = 0.01). This observation is consistent with previous findings related to the transmission of dual-tropic HIV produced in macrophages versus CD4+ T cells through DC-SIGN [20]. Similarly, DC-SIGNR and Langerin preferentially transferred M-SIV in comparison to T-SIV (t-test, p = 0.0001, 0.0003). These findings suggest that SIV replication in macrophages produces viral particles with distinctive characteristics that confer a clear advantage in direct and possibly indirect viral spread via lectins compared to viruses originating from CD4+ T cells.

Host cell-dependent features of SIV define the sensitivity to carbohydrate binding agents (CBAs) and neutralizing antibodies

CBAs bind glycan structures, such as those present on viral envelope proteins. Within the realm of antiviral activity against HIV, CBAs encompass a range of compounds including lectins, certain glycan-binding broadly neutralizing antibodies, and the nonpeptidic antibiotic Pradimicin A [32]. Consequently, next to non-glycan dependent broadly neutralizing antibodies, CBAs are viewed as promising biomedical treatments for preventing the transmission of HIV [32,33]. Due to the observed differences in *N*-glycomes between M-SIV and T-SIV, it was plausible that host cell-derived features of SIV Env might influence the effectiveness of CBAs and neutralizing antibodies. To explore this hypothesis, we examined the ability of CBAs to inhibit SIV infection of TZM-bl cells, the standard indicator cell line for neutralization assays in the field of HIV research [34]. In these experiments, we focused on two glycan species groups: oligomannose-type glycans and core fucosylated complex-type glycans, which were incorporated in different quantities into M-SIV and T-SIV gp120 (Fig 1D). In these experiments, we included HIV-1 Env as a reference protein and the vesicular stomatitis virus glycoprotein (VSV-G), which contains only two *N*-glycosylation signals per protomer [35] and thus should be non- or little sensitive to inhibition by CBA. VSV-G further differs from HIV/SIV Env by mediating fusion with the endosomal and not the plasma membrane [36]. In our experiments, the pre-treatment with ulex europaeus agglutinin (UEA), a lectin against core fucose, did not interfere with the infection of TZM-bl cells by controls (HIV-1 or VSV-G pseudotyped viruses) or SIV (Fig 3A) as expected [37]. As anticipated, HIV-1 was highly sensitive to inhibition by mannose-specific lectins cyanovirin-N (CV-N, target: Manα1–2) or galanthus nivalis agglutinin (GNA, target: Manα1–3, Manα1–6), while there was significantly less inhibition of infection by pseudotypes bearing the minimally glycosylated protein VSV-G [38,39]. Consistent with the western blot and xCGE-LIF data (Fig 1B and 1D), T-SIV with its apparently higher oligomannose content in gp120 was more strongly inhibited than M-SIV in a concentration-dependent manner (Fig 3A), and these differences were statistically significant (Fig 3B, t-test, CV-N: p = 0.0032, GNA: p = 0.008). Thus, the producer cell type can influence SIV susceptibility to inhibition by mannose-specific CBAs.

To investigate whether cell type-dependent differences in SIV impact antibody neutralization effectiveness, we conducted infections of TZM-bl cells with HIV, M-SIV, and T-SIV in the presence of neutralizing sera. These sera were obtained from rhesus macaques infected with SIVmac239, the parental strain of SIVmac239/316 Env used for producing M- and T-SIV. This parental virus differs in nine amino acids, making it more resistant to antibody neutralization [24]. Using four different sera, we observed some inhibition of HIV (Fig 3C). Intriguingly, M-SIV was neutralized more efficiently than T-SIV. These effects were concentration-dependent (Fig 3D) and statistically significant (Fig 3E, paired t-test, p = 0.013). In light of these findings, we conclude that differences originating from the virus-producing cell can influence the efficacy of CBA and antibody neutralization, and thus might have relevance for the development of biomedical interventions based on these scaffolds.
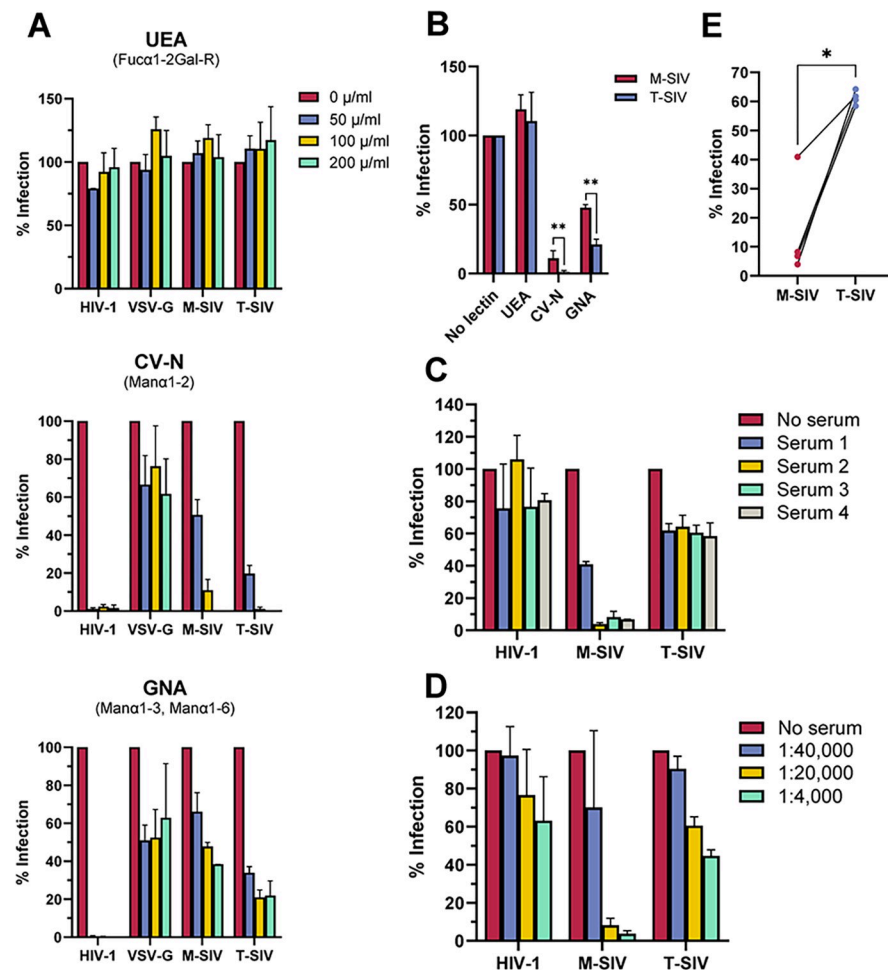
Fig 3. T-SIV is more sensitive to inhibition by mannose-specific lectins, while M-SIV is more efficiently neutralized by sera. A) Infectivity-normalized M-SIV, T-SIV, HIV-1 NL4-3 and *env*-defective HIV-1 NL4-3 pseudotyped with vesicular stomatitis virus glycoprotein (VSV-G) were preincubated with the indicated concentrations of ulex europaeus agglutinin (UEA), cyanovirin-N (CV-N), or galanthus nivalis agglutinin (GNA), before addition to TZM-bl indicator cells. Virus was removed at 5–6 h post infection and β–galactosidase activity was measured in cell lysates at 72 h post infection. Presented are the grand mean values with SEM normalized to lectin-free conditions from two independent experiments conducted in triplicates for all lectin concentrations. B) Plotted are the results obtained in A) for M-SIV and T-SIV using a lectin concentration of 100 µg/ml. Statistical differences between M-SIV and T-SIV were calculated for each lectin using a paired t-test (**, p ≤ 0.01). C) Infectivity-normalized M-SIV, T-SIV, and HIV-1 NL4-3 were preincubated with sera from SIVmac239-infected rhesus macaques at varying dilutions prior to infection of TZM-bl indicator cells. Incubation of virus with medium alone served as negative control. Virus removal occurred at 5–6 hours post-infection, with β-galactosidase activity measured in cell lysates at 72 hours post-infection. Shown is the grand mean with SEM from two independent experiments conducted in triplicates at a serum dilution of 1:20,000. Infection in the absence of serum was normalized to 100%. D) The titration curve for serum 3 from C) is presented as grand mean with SEM. E) Data for sera 1–4 from C), all at a 1:20,000 dilution, are directly compared. Paired t-test was applied to assess differences in means between groups (*, p ≤ 0.05).

https://doi.org/10.1371/journal.ppat.1012190.g003

Discussion

Here, we analyzed whether isogenic macrophage-tropic SIV produced in primary rhesus macaque macrophages (M-SIV) or CD4+ T cells (T-SIV) differs in Env glycosylation, viral spread and neutralization sensitivity. We found that the overall glycan landscape of M-SIV and T-SIV gp120 shared similarities; however, different quantities of the glycan species were incorporated. Oligomannose-type *N*-glycans were more frequent in T-SIV gp120 and the

complex glycan profiles between both viruses varied considerably, although our study was insufficiently powered to determine whether these differences were statistically significant. The producer cell type influenced viral infectivity, with M-SIV being more infectious and being better transmitted by lectin-expressing cells as compared to T-SIV. The host cell type also affected viral sensitivity to CBAs and neutralizing antibodies, with T-SIV showing greater sensitivity to inhibition by mannose-specific lectins and M-SIV being more efficiently neutralized by antibodies.

CD4+ T cell-derived viruses exhibit a greater prevalence of oligomannose structures in gp120 [19,21] but less LacdiNac residues in comparison to virus originating from macrophages [15]. By providing the first comparative molecular analysis of gp120 glycosylation of primary host cells, we corroborate and expand upon these earlier observations. Our xCGE-LIF analysis indicated an increased presence of oligomannose-type N-glycans with 5, 6, and 8 mannose residues on T-SIV-derived gp120 in comparison to M-SIV-derived gp120. The signature for the oligomannose-type N-glycan with 9 mannose residues (Man9) also appeared to be elevated in T-SIV versus M-SIV. However, it is important to note that this study did not allow for a definitive conclusion due to the potential co-migration of Man9 with another N-glycan structure (FA2G2). Nevertheless, other studies indicated that Man9 is a frequently incorporated glycan species, or even the predominant one, in CD4+ T cell-derived HIV gp120 [40,41]. Beyond differential LacdiNac incorporation, we observed additional variations in the complex glycan profiles of T-SIV and M-SIV, which align with the expectations generated by an mRNA analysis of more than 20 glycosylation-related enzymes in CD4+ T cells and macrophages [19]. Specifically, rhesus macaque CD4+ T cells exhibit elevated expression levels of genes that potentially enhance core fucosylation (FUT8) and sialylation (ST6Gal1), while rhesus macaque macrophages express higher levels of genes that promote the conversion of oligomannose to complex glycans (MGAT1), a reduction in sialic acid (NPL), and high-level branching (MGAT4B) [19].

The advantages observed for M-SIV over T-SIV in terms of direct and indirect viral spread prompt the question of whether these differences could lead to more efficient *in vivo* transmission of macrophage-derived viruses. It is noteworthy that SIVmac239/316 Env produced in macrophages exhibited traits similar to those reported for HIV-1 transmitted founder viruses when compared to unmatched chronic isolates. In this study, transmitted founder viruses showed increased Env incorporation, higher infectivity, and enhanced transfer to target cells by DCs in comparison to chronic viral isolates [42]. Similarly, SIVmac239/316 Env replicated to higher levels in CD4+ T cells as compared to macrophages and M-SIV incorporated more Env, was displaying higher infectivity, and was better transmitted by (DC) lectins than T-SIV. This suggests that macrophage origin might strengthen viral characteristics associated with successful viral transmission. Furthermore, one of our previous studies using SIVmac239/316 Env and the rhesus macaque model indicated that exclusive oligomannose glycosylation of Env completely prevents *in vivo* SIV transmission [37], suggesting that the oligomannose glycan content of CD4+ T cell-derived HIV and SIV may be unfavorable during sexual transmission. While our exploratory animal experiment showed that the oligomannose profile of T-SIV Env did not have the same detrimental effect on virus transmission as observed for exclusive oligomannose glycosylation, larger animal studies might decipher potential differences in the *in vivo* transmissibility of macrophage and CD4+ T cell-derived viruses. Thus, macrophage-dependent viral traits such as the Env glycosylation profile might booster virus dissemination.

Our results support the conclusions of others that cell type-dependent differences in HIV and SIV influence the sensitivity towards potential biological interventions including lectins and antibodies [15,16,20]. In contrast to our results, two other studies determined

macrophage-derived HIV to be more neutralization sensitive than viruses produced in CD4+ T cells [15,20]. While one study utilized HIV and 2G12, a mannose-only binding neutralizing antibody, for their investigations [20], the other study made this conclusion by using sera of an HIV infected chimpanzee [15]. This suggests that whether macrophage or CD4+ T cell-derived traits provide protection for the virus *in vivo*, is likely dependent on the specific antibody profile of the host. Although host cell-dependent differences appear to be important for antibody and lectin interactions *in vitro*, these might have a negligible relevance *in vivo*, considering that CD4+ T cells are likely the main virus producing cells over the course of infection [43]. Future research must determine whether host cell-dependent viral distinctions should factor into the selection of candidate therapeutics and the design of strategies to address the challenges posed by the extensive diversity of HIV.

One limitation of this study is the use of a single SIV strain, which was carefully chosen from the few available macrophage-tropic SIV proviruses previously used in studies with rhesus macaques. Since the completion of our study, HIV strains were found to differ in their sensitivity to host cell-derived modifications of their traits [20], emphasizing the need for testing multiple viral strains for more comprehensive conclusions. Additionally, limited blood availability from rhesus macaques constrained the production of sufficient virus for extended glycan analysis, preventing the identification of overlapping peaks in xCGE-LIF annotations via glycosidase digest. Finally, host cell-dependent glycosylation differences in Env might explain the observed variations in viral functions [19–21]. However, other factors such as viral surface glycosylation beyond Env [44], host cell protein incorporation [45,46], and virus stock impurities like exosomes [47] could have influenced the presented results.

In summary, using SIV as a model for HIV we provide the first detailed molecular characterization of gp120 *N*-glycomes as derived by the target cells macrophages and CD4+ T cells. Further, our findings highlight the significance of host cell-dependent differences, affecting viral spread and neutralization sensitivity. Overall, our findings might have broader implications for the successful development of innovative strategies for HIV prevention and therapy.

Material and methods

All data underpinning this study, which is not already included in the manuscript, are publicly available at Dryad (https://datadryad.org/stash) with the identifier doi:10.5061/dryad.hmgqnk9rm [48].

Ethics statement

The animal studies were conducted at the German Primate Center, which has the permission to breed and house non-human primates under license number 392001/7 granted by the veterinary office of the city Göttingen and conforming with x 11 of the German Animal Welfare act. Approval was obtained from the ethics committee of the Lower Saxony State Office for Consumer Protection and Food Safety with the project license 33.14-42502-04-11/026. All animals were bred, cared for by qualified staff and, housed at the German Primate Center adhering to the German Animal Welfare Act and complying with the European Union guidelines for the use of nonhuman primates in biomedical research.

Animal studies

In total, eight male and one female Indian-origin rhesus macaques (*Macaca mulatta*) were assigned to experimental groups based on their age (4 to 7 years). A maximum of 5–6 ml blood per kg bodyweight was drawn *ex vivo* from animals, which were anesthetized intramuscularly with 10 mg ketamine per kg body weight from the femoral vein employing the

Vacutainer system (BD Biosciences). For virus challenges, animals were anesthetized intra-muscularly with a mixture of 5 mg ketamine, 1 mg xylazin, and 0.01 mg atropine per kg body weight. Virus introduction occurred up to ten centimeters into the rectum using a catheter (Urotech). During the procedure and for the subsequent 30 minutes, the animals were maintained in a ventral position with an elevated pelvis. Monitoring for infection establishment by RT-PCR took place every two and three weeks post-challenge.

All data underpinning this study, which is not already included in the manuscript, are publicly available at Dryad (https://datadryad.org/stash) with the identifier doi:10.5061/dryad.hmgqnk9rm [48].

Plasmids

The plasmids encoding HIV-1 NL4-3 [27], SIVmac239/316 Env [22], the HIV-1 NL4-3-derived vector pNL4-3.Luc.R-E- [49], and the vesicular stomatitis virus glycoprotein [50] have been previously described.

Cell culture

293T and TZM-bl cells were cultured in Dulbecco's modified Eagle's medium (DMEM; PAN-Biotech) supplemented with 10% fetal bovine serum (FBS, Biochrome), 100 U/ml penicillin, and 100 µg/ml streptomycin (P/S; PAN-Biotech). The suspension cell lines (C8166, CEMx174 R5, Raji, Raji DC-SIGN/DC-SIGNR/Langerin) were cultured in RPMI 1640 supplemented with L-glutamine (PAN-Biotech), 10% FBS, and P/S. For the isolation of rhesus macaque primary CD4⁺ T cells and macrophages, PBMCs were isolated from whole blood using ficoll (Biochrom) density gradient centrifugation. CD4⁺ T cells were purified by negative depletion using magnetic microbeads (Miltenyi Biotech) following the manufacturer's protocol and cultured in RPMI 1640 supplemented with 20% FBS, P/S and 10 µg/ml concanavalin A (Sigma-Aldrich) for 24 h at a density of 2×10^6 cells/ml. Following that, CD4⁺ T cells were cultured in RPMI 1640 supplemented with 20% FBS, P/S and 100 U/ml recombinant human interleukin-2 (IL-2). For the generation of macrophages, monocytes were purified from PBMCs by positive selection for CD14⁺ cells with magnetic microbeads (Miltenyi Biotech) following the manufacturer's protocol. For differentiation into macrophages, monocytes were seeded at a density of 3×10^5 cells/ml in RPMI 1640 medium supplemented with 20% FBS, 10% human AB serum (Sigma-Aldrich), and 10 ng/ml recombinant human macrophage colony stimulating factor (Peprotech). The medium was replenished after 2 d and the cells differentiated for a total of 5 d. Subsequently, macrophages were cultured in RPMI 1640 supplemented with 20% FBS. All cells were grown in a humidified atmosphere at 37°C with 5% CO_2.

Flow cytometry

For flow cytometric analysis of marker expression, 50,000 to 500,000 PBMCs and the above mentioned cell subsets were stained for 30 min at room temperature (RT) with mixtures of monoclonal antibodies (mAb) reactive against CD3 (SP34-2, Alexa Fluor 700), CD4 (L200, V450), CD11b (ICRF44, PE), CD16 (3G8, FITC) and CD20 (L27, PE-Cy7) all from BD Biosciences, as well as CD8 (3B5, Pacific Orange, Invitrogen), and CD14 (RMO52, ECD, Beckman Coulter) diluted in staining buffer (phosphate-buffered saline with 5% FBS). Subsequently, cells were washed with staining buffer, and fixed with 4% paraformaldehyde solution for seven minutes. After an additional washing step, the cells were analyzed using a LSRII cytometer (BD Biosciences) equipped with three lasers. Compensation was calculated by FACS DIVA software 6.1.3 using appropriate single antibody labeled compensation beads from Sphero-Tech. Data analysis was performed using FlowJo software v9.6 (Treestar).

Production of viruses and pseudotyped viruses

To generate virus stocks of HIV-1 NL4-3 and SIVmac239/316 Env, 293T cells were seeded into T25-cell culture flasks and transfected with 12 μg of plasmids encoding proviral DNA using calcium phosphate. For pseudotype production, 293T cells were cotransfected with plasmids encoding pNL4-3.Luc.R-E- and VSV-G. The culture medium was exchanged at 6–7 h post transfection, and the cellular supernatant was harvested at 72 h post transfection. The supernatants were clarified from debris by centrifugation (5 min, 3488 x g, RT) filtered through a 0.45 μm filter, aliquoted and stored at -80˚C.

Amplification of SIV in T cells and macrophages

To produce SIVmac239/316 Env in CD4+ T cells, the concanavalin A stimulated cells were infected with SIVmac239/316 Env generated in 293T cells at a multiplicity of infection (MOI) of 0.1 in RPMI 1640 medium supplemented with 20% FCS and P/S at RT under occasional shaking. Subsequently, the cells were grown in medium supplemented with IL-2 and incubated for 48 h. The cells were then washed twice with 5 ml of culture medium, transferred to a new cell culture flask, and cultured for 2 weeks. Every 2–3 d, the cells were pelleted, the supernatant was harvested and the cells were dissolved in fresh media at a density of 2×10^6 cells/ml. The supernatants were processed as described above for pseudotypes and viral capsid protein concentration determined by a p27-antigen capture enzyme linked immunosorbent assay (ABL), following the manufacturer's instructions. The p27-antigen-positive supernatants from CD4+ T cell cultures obtained from 9 donor animals were pooled to create the stock of CD4+ T cell-derived SIVmac239/316 Env, referred to as T-SIV throughout the manuscript. To generate SIVmac239/316 Env in macrophages (M-SIV), the same procedure as described above was followed, except that washing and harvesting of the cells were conducted without detaching the cells from the cell culture flask, and no IL-2 was added to the cell culture medium. The M-SIV virus stock was derived from infected cultures established from eight donor animals. To confirm the absence of mutations in env introduced during virus replication, we isolated RNA from M-SIV and T-SIV using the High Pure Viral RNA Kit (Roche), converted it to cDNA with the Cloned AMV First-Strand cDNA Synthesis Kit (Invitrogen), and then sequenced it after PCR amplification. The viral stocks were further characterized for p27-capsid content, as described above, and for infectious units/ml by titration on C8166 cells as described before [51].

Infectivity assays

For the determination of virus stock infectivity, TZM-bl cells, the standard indicator cell line for neutralization assays using clinical samples [34], were utilized. The cells were seeded at a density of 10,000 cells per well in a 96-well cell culture plate and allowed to adhere for 2 hours prior to infection. Infection was carried out using p27-capsid protein or MOI normalized SIVmac239/316 Env in a total volume of 100 μl. After 2 h of spin-oculation (870 x g, RT) [52], the infection was allowed to continue for 3–4 h at 37˚C. Thereafter, the infection medium was replaced by 200 μl of fresh culture medium and the cells were cultured for 72 h. Subsequently, the cells were lysed and beta-galactosidase activity in lysates was detected using a commercially available kit (Applied Biosystem) following the manufacturer's protocol. For lectin inhibition assays, infectivity normalized M-SIV, T-SIV, HIV-1 NL4-3 and env-defective NL4-3 pseudotyped with VSV-G were preincubated with PBS or the lectins UEA (Eylabs), GNA (Sigma), or CV-N [38] for 15 min at 37˚C. Subsequently, the lectin-virus mix was added to TZM-bl cells for infection, and the infection efficiency was determined as described earlier. To assess antibody-mediated neutralization, a similar experimental procedure as the lectin inhibition assay

was carried out, except that sera obtained from SIVmac239-infected rhesus macaques were used instead of lectins. Before use, the sera were heat-inactivated for 30 minutes at 56˚C.

Transmission assays

To model viral transmission we followed a previously published protocol [31]. Briefly, 30,000 Raji, Raji DC-SIGN, Raji DC-SIGNR, or Raji Langerin cells were preincubated for 2–3 h at 37˚C with virus adjusted to ensure equivalent infectivity on the CEMx174 R5 target cell line. Subsequently, the cells underwent two washes with 5 ml PBS each (270 x g, 5 min) to eliminate unbound virus. Following this, the cells were co-cultured with 30,000 CEMx174 R5 target cells in 100 μl of RPMI-1640 medium in a 96-well cell culture plates. After two days, 50 μl of the medium was replaced with fresh media. One day thereafter, the cells were lysed, and luciferase activity was quantified utilizing a commercially available assay kit (Promega). In addition, all cell lines were infected directly without subsequent removal of unbound viruses to control the uniform infectivity of viruses and background signals of transmitter cell lines.

Western blot

For the analysis of viral particle content, the virus was concentrated through a 20% sucrose cushion in TNE buffer (0.01 M Tris-HCl pH 7.4, 0.15 M NaCl and 2 mM EDTA in ddH$_2$O) using centrifugation. The proteins from the pelleted virions were then separated using SDS-PAGE and subjected to western blot analysis. SIV gp120 was detected using the mouse monoclonal gp120-specific antibody DA6 [53] at a dilution of 1:2,000, while the mouse mono-clonal p27-specific antibody 55-2F12 [54] was employed at a dilution of 1:100 for the detection of p27-capsid protein. As a secondary antibody, a horseradish peroxidase-labeled antibody of appropriate species specificity from Dianova was employed at a dilution of 1:5,000. In order to examine the glycosylation of gp120, the concentrated virus was treated with either Endo H or PNGase F from New England Biolabs, for 30 min prior to SDS-PAGE. Signal intensities of western blot bands were quantified using the software ImageJ [55].

Glycoprofiling by xCGE-LIF

To investigate the *N*-glycosylation of gp120 from M- and T-SIV, sample preparation and analysis were performed as described before [56]. Briefly, the virions were concentrated by ultra-centrifugation through a sucrose cushion and the viral proteins were separated by SDS-PAGE. The gp120 protein bands were excised from the Coomassie Blue-stained SDS-polyacrylamide gels, destained, reduced, and alkylated. The attached *N*-glycans were then released by in-gel incubation with PNGase F, and the released *N*-glycans were extracted with water. Next, the *N*-glycans were labeled with 8-aminopyrene-1,3,6-trisulfonic acid (APTS), and any excess label was removed using hydrophilic interaction solid phase extraction. The fluorescently labeled *N*-glycans were separated and analyzed by xCGE-LIF. The glyXtoolCE software (glyXera) was utilized to process the data generated by xCGE-LIF, including the normalization of migration times to an internal standard. This resulted in the creation of *N*-glycan "fingerprints" where the signal intensity in relative fluorescence units (RFU) was plotted on the y-axis against the aligned migration time in aligned migration time units (MTU") on the x-axis. The high repro-ducibility of aligned migration times allowed for the comparison of *N*-glycan "fingerprints" between different samples. To elucidate the *N*-glycan structures and annotate the peaks, an in-house *N*-glycan database was used. For quantitative comparison, the relative peak height, which represents the ratio of the peak height to the total height of all peaks, was calculated for each peak and sample.

LC-MS/MS and automated MS data analysis

After the in-gel release of *N*-glycans by PNGase F treatment proteins were digested with trypsin according to the method outlined by Shevchenko *et al.* [57]. The procedure involved reducing the proteins with 10 mM DTT (Sigma-Aldrich), followed by carbamidomethylation with 100 mM iodocetamide (Sigma-Aldrich), and subsequent digestion with sequencing-grade trypsin (Promega). To extract the resulting peptides, acetonitrile was used, and the samples were then dried in a vacuum centrifuge before being dissolved in a solution containing 2% (v/v) acetonitrile and 0.1% (v/v) trifluoroacetic acid (Sigma-Aldrich) for subsequent LC-MS/MS analysis. The analysis was performed using a LTQ-Orbitrap Velos mass spectrometer (Thermo Fisher Scientific) coupled online to a nano-flow ultra-high-pressure liquid chromatography system (RSLC, Thermo Fisher Scientific). Reverse-phase chromatography and mass spectrometry was carried out as described previously [58]. For data analysis, the MaxQuant proteomics software suite version 1.2.2.5 [59] was utilized, and peak lists were searched against the SIV-mac239/316 Env sequence using the Andromeda search engine version 1.1.0.36 [60].

Software

Graphs and statistics were conducted using the GraphPad Prism 9 (Dotmatics) software unless stated otherwise. The text of this manuscript was subjected to rephrasing using ChatGPT (OpenAI) to enhance its linguistic quality.

Supporting information

S1 Fig. Exemplary flow cytometric validation of purified CD4+ T cells and macrophages. A) Rhesus macaque PBMCs and monocyte-derived macrophages were flow cytometrically stained using antibodies targeting macrophage (CD11b, CD14, CD16), T cell (CD3), and B cell (CD20) markers. Representative data from four different experiments are presented. B) Rhesus macaque PBMCs or purified CD4+ T cells were stained for flow cytometry using antibodies specific for T cells (CD3) or T cell subpopulations (CD4, CD8). Representative data from two independent experiments are shown. For A) and B), the y-axis represents the cell count, while the x-axis indicates marker signal intensity. Proportions of cells within gates are denoted above the bars.
(TIF)

S2 Fig. Structures and relative intensities of *N*-glycans derived from M-SIV and T-SIV, analyzed by xCGE-LIF. Relative peak abundances are presented as percentages of the total peak intensity (peaks 1–96 = 100%). *N*-glycan structures were assigned to peaks based on migration times matching the entries of an in-house *N*-glycan database. Symbols used to depict *N*-glycan structures are given in Fig 1A.
(TIF)

S3 Fig. Both M-SIV and T-SIV are infectious *in vivo*. A) Rhesus macaques (n = 4–5 per group) were rectally challenged with 3 ng p27-capsid-protein of M-SIV or T-SIV diluted in PBS. The challenges were repeated every three weeks until the animals became infected (indicated by black filled symbols) or up to six challenges. Infection was determined by detection of SIV RNA in the peripheral blood by quantitative reverse transcriptase-polymerase chain reaction (RT-PCR). Animal identifiers are indicated on the y-axis. B) Plasma viral load of rhesus macaques infected with M-SIV or T-SIV was measured as RNA copies/ml from the day of challenge (day 0) up to 10 weeks post infection (wpi). At 3 wpi with SIVmac239/316 Env, animal 13057 underwent an additional challenge with SIVmac251 as part of a separate

experiment, which was not part of this study.
(TIF)

Acknowledgments

Author Contributions

Conceptualization: Rita Gerardy-Schahn, Stefan Pöhlmann.

Data curation: Christina B. Karsten, Samanta Cajic, Berit Roshani, Antonina Klippert, Ulrike Sauermann, Christiane Stahl-Hennig.

Formal analysis: Christina B. Karsten, Falk F. R. Buettner, Samanta Cajic, Berit Roshani, Antonina Klippert, Ulrike Sauermann, Christiane Stahl-Hennig, Stefan Pöhlmann.

Funding acquisition: Rita Gerardy-Schahn, Stefan Pöhlmann.

Investigation: Christina B. Karsten, Falk F. R. Buettner, Samanta Cajic, Inga Nehlmeier, Berit Roshani, Antonina Klippert, Nicole Stolte-Leeb, Christiane Stahl-Hennig.

Methodology: Christina B. Karsten, Falk F. R. Buettner, Berit Roshani, Antonina Klippert, Erdmann Rapp, Christiane Stahl-Hennig, Stefan Pöhlmann.

Project administration: Christina B. Karsten, Udo Reichl, Erdmann Rapp, Christiane Stahl-Hennig.

Resources: Rita Gerardy-Schahn, Erdmann Rapp, Christiane Stahl-Hennig.

Supervision: Rita Gerardy-Schahn, Stefan Pöhlmann.

Validation: Christina B. Karsten, Falk F. R. Buettner, Samanta Cajic, Ulrike Sauermann, Erdmann Rapp, Christiane Stahl-Hennig, Stefan Pöhlmann.

Visualization: Christina B. Karsten, Samanta Cajic, Berit Roshani, Antonina Klippert, Christiane Stahl-Hennig, Stefan Pöhlmann.

Writing – original draft: Christina B. Karsten, Stefan Pöhlmann.

Writing – review & editing: Christina B. Karsten, Falk F. R. Buettner, Samanta Cajic, Inga Nehlmeier, Berit Roshani, Antonina Klippert, Ulrike Sauermann, Nicole Stolte-Leeb, Udo Reichl, Rita Gerardy-Schahn, Erdmann Rapp, Christiane Stahl-Hennig, Stefan Pöhlmann.

References

1. UNAIDS. Fact sheet 2023: Global HIV/AIDS Statistics: UNAIDS; 2023 [updated 2023 July 13]. Available from: https://www.unaids.org/en/resources/documents/2023/UNAIDS_FactSheet.

2. Walsh SR, Seaman MS. Broadly Neutralizing Antibodies for HIV-1 Prevention. Front Immunol. 2021; 12:712122. Epub 20210720. https://doi.org/10.3389/fimmu.2021.712122 PMID: 34354713; PubMed Central PMCID: PMC8329589.

3. Hallenberger S, Bosch V, Angliker H, Shaw E, Klenk HD, Garten W. Inhibition of furin-mediated cleavage activation of HIV-1 glycoprotein gp160. Nature. 1992; 360(6402):358–61. https://doi.org/10.1038/360358a0 PMID: 1360148.

4. Chen B. Molecular Mechanism of HIV-1 Entry. Trends Microbiol. 2019; 27(10):878–91. Epub 2019/07/03. https://doi.org/10.1016/j.tim.2019.06.002 PMID: 31262533; PubMed Central PMCID: PMC6744290.

5. Zhu X, Borchers C, Bienstock RJ, Tomer KB. Mass spectrometric characterization of the glycosylation pattern of HIV-gp120 expressed in CHO cells. Biochemistry. 2000; 39(37):11194–204. Epub 2000/09/14. https://doi.org/10.1021/bi000432m PMID: 10985765.

6. Wei X, Decker JM, Wang S, Hui H, Kappes JC, Wu X, et al. Antibody neutralization and escape by HIV-1. Nature. 2003; 422(6929):307–12. https://doi.org/10.1038/nature01470 PMID: 12646921.

7. Geijtenbeek TB, Kwon DS, Torensma R, van Vliet SJ, van Duijnhoven GC, Middel J, et al. DC-SIGN, a dendritic cell-specific HIV-1-binding protein that enhances trans-infection of T cells. Cell. 2000; 100 (5):587–97. https://doi.org/10.1016/s0092-8674(00)80694-7 PMID: 10721995.

8. Quinones-Kochs MI, Buonocore L, Rose JK. Role of N-linked glycans in a human immunodeficiency virus envelope glycoprotein: effects on protein function and the neutralizing antibody response. J Virol. 2002; 76(9):4199–211. Epub 2002/04/05. https://doi.org/10.1128/jvi.76.9.4199-4211.2002 PMID: 11932385; PubMed Central PMCID: PMC155056.

9. Ma BJ, Alam SM, Go EP, Lu X, Desaire H, Tomaras GD, et al. Envelope deglycosylation enhances antigenicity of HIV-1 gp41 epitopes for both broad neutralizing antibodies and their unmutated ancestor antibodies. PLoS Pathog. 2011; 7(9):e1002200. Epub 20110901. https://doi.org/10.1371/journal.ppat.1002200 PMID: 21909262; PubMed Central PMCID: PMC3164629.

10. Koch M, Pancera M, Kwong PD, Kolchinsky P, Grundner C, Wang L, et al. Structure-based, targeted deglycosylation of HIV-1 gp120 and effects on neutralization sensitivity and antibody recognition. Virology. 2003; 313(2):387–400. https://doi.org/10.1016/s0042-6822(03)00294-0 PMID: 12954207.

11. Reitter JN, Means RE, Desrosiers RC. A role for carbohydrates in immune evasion in AIDS. Nat Med. 1998; 4(6):679–84. Epub 1998/06/12. https://doi.org/10.1038/nm0698-679 PMID: 9623976.

12. Johnson WE, Sanford H, Schwall L, Burton DR, Parren PW, Robinson JE, Desrosiers RC. Assorted mutations in the envelope gene of simian immunodeficiency virus lead to loss of neutralization resistance against antibodies representing a broad spectrum of specificities. J Virol. 2003; 77(18):9993–10003. Epub 2003/08/28. https://doi.org/10.1128/jvi.77.18.9993-10003.2003 PMID: 12941910; PubMed Central PMCID: PMC224602.

13. Stanley P, Moremen KW, Lewis NE, Taniguchi N, Aebi M. N-Glycans. In: Varki A, Cummings RD, Esko JD, Stanley P, Hart GW, Aebi M, et al., editors. Essentials of Glycobiology. 4. Cold Spring Harbor (NY): Cold Spring Harbor Laboratory Press; 2022. p. 103–16.

14. Pritchard LK, Vasiljevic S, Ozorowski G, Seabright GE, Cupo A, Ringe R, et al. Structural Constraints Determine the Glycosylation of HIV-1 Envelope Trimers. Cell Rep. 2015; 11(10):1604–13. Epub 20150604. https://doi.org/10.1016/j.celrep.2015.05.017 PMID: 26051934; PubMed Central PMCID: PMC4555872.

15. Willey RL, Shibata R, Freed EO, Cho MW, Martin MA. Differential glycosylation, virion incorporation, and sensitivity to neutralizing antibodies of human immunodeficiency virus type 1 envelope produced from infected primary T-lymphocyte and macrophage cultures. J Virol. 1996; 70(9):6431–6. Epub 1996/09/01. https://doi.org/10.1128/JVI.70.9.6431-6436.1996 PMID: 8709276; PubMed Central PMCID: PMC190674.

16. Raska M, Takahashi K, Czernekova L, Zachova K, Hall S, Moldoveanu Z, et al. Glycosylation patterns of HIV-1 gp120 depend on the type of expressing cells and affect antibody recognition. J Biol Chem. 2010; 285(27):20860–9. Epub 2010/05/05. https://doi.org/10.1074/jbc.M109.085472 PMID: 20439465; PubMed Central PMCID: PMC2898351.

17. Liedtke S, Adamski M, Geyer R, Pfützner A, Rübsamen-Waigmann H, Geyer H. Oligosaccharide profiles of HIV-2 external envelope glycoprotein: dependence on host cells and virus isolates. Glycobiology. 1994; 4(4):477–84. https://doi.org/10.1093/glycob/4.4.477 PMID: 7827409.

18. Liedtke S, Geyer R, Geyer H. Host-cell-specific glycosylation of HIV-2 envelope glycoprotein. Glycoconj J. 1997; 14(7):785–93. https://doi.org/10.1023/a:1018577619036 PMID: 9511983.

19. Gaskill PJ, Zandonatti M, Gilmartin T, Head SR, Fox HS. Macrophage-derived simian immunodeficiency virus exhibits enhanced infectivity by comparison with T-cell-derived virus. J Virol. 2008; 82 (3):1615–21. Epub 2007/11/30. https://doi.org/10.1128/JVI.01757-07 PMID: 18045942; PubMed Central PMCID: PMC2224434.

20. Heeregrave EJ, Thomas J, van Capel TM, de Jong EC, Pollakis G, Paxton WA. Glycan dependent phenotype differences of HIV-1 generated from macrophage versus CD4(+) T helper cell populations. Front Immunol. 2023; 14:1107349. Epub 20230621. https://doi.org/10.3389/fimmu.2023.1107349 PMID: 37415979; PubMed Central PMCID: PMC10320205.

21. Lin G, Simmons G, Pohlmann S, Baribaud F, Ni H, Leslie GJ, et al. Differential N-linked glycosylation of human immunodeficiency virus and Ebola virus envelope glycoproteins modulates interactions with DC-SIGN and DC-SIGNR. J Virol. 2003; 77(2):1337–46. Epub 2002/12/28. https://doi.org/10.1128/jvi.77.2.1337-1346.2003 PMID: 12502850; PubMed Central PMCID: PMC140807.

22. Mori K, Ringler DJ, Kodama T, Desrosiers RC. Complex determinants of macrophage tropism in env of simian immunodeficiency virus. J Virol. 1992; 66(4):2067–75. https://doi.org/10.1128/JVI.66.4.2067-2075.1992 PMID: 1548752; PubMed Central PMCID: PMC288997.

23. Mori K, Ringler DJ, Desrosiers RC. Restricted replication of simian immunodeficiency virus strain 239 in macrophages is determined by env but is not due to restricted entry. J Virol. 1993; 67(5):2807–14. https://doi.org/10.1128/JVI.67.5.2807-2814.1993 PMID: 7682627; PubMed Central PMCID: PMC237605.

24. Puffer BA, Pöhlmann S, Edinger AL, Carlin D, Sanchez MD, Reitter J, et al. CD4 independence of simian immunodeficiency virus Envs is associated with macrophage tropism, neutralization sensitivity, and attenuated pathogenicity. J Virol. 2002; 76(6):2595–605. https://doi.org/10.1128/jvi.76.6.2595-2605.2002 PMID: 11861825; PubMed Central PMCID: PMC135960.

25. Mori K, Rosenzweig M, Desrosiers RC. Mechanisms for adaptation of simian immunodeficiency virus to replication in alveolar macrophages. J Virol. 2000; 74(22):10852–9. https://doi.org/10.1128/jvi.74.22.10852-10859.2000 PMID: 11044136; PubMed Central PMCID: PMC110966.

26. Li Y, Luo L, Rasool N, Kang CY. Glycosylation is necessary for the correct folding of human immunodeficiency virus gp120 in CD4 binding. J Virol. 1993; 67(1):584–8. Epub 1993/01/01. https://doi.org/10.1128/JVI.67.1.584-588.1993 PMID: 8416385; PubMed Central PMCID: PMC237399.

27. Pöhlmann S, Baribaud F, Lee B, Leslie GJ, Sanchez MD, Hiebenthal-Millow K, et al. DC-SIGN interactions with human immunodeficiency virus type 1 and 2 and simian immunodeficiency virus. J Virol. 2001; 75(10):4664–72. https://doi.org/10.1128/JVI.75.10.4664-4672.2001 PMID: 11312337; PubMed Central PMCID: PMC114220.

28. de Witte L, Nabatov A, Pion M, Fluitsma D, de Jong MA, de Gruijl T, et al. Langerin is a natural barrier to HIV-1 transmission by Langerhans cells. Nat Med. 2007; 13(3):367–71. Epub 20070304. https://doi.org/10.1038/nm1541 PMID: 17334373.

29. Bashirova AA, Geijtenbeek TB, van Duijnhoven GC, van Vliet SJ, Eilering JB, Martin MP, et al. A dendritic cell-specific intercellular adhesion molecule 3-grabbing nonintegrin (DC-SIGN)-related protein is highly expressed on human liver sinusoidal endothelial cells and promotes HIV-1 infection. J Exp Med. 2001; 193(6):671–8. https://doi.org/10.1084/jem.193.6.671 PMID: 11257134; PubMed Central PMCID: PMC2193415.

30. Gonzalez SM, Aguilar-Jimenez W, Su RC, Rugeles MT. Mucosa: Key Interactions Determining Sexual Transmission of the HIV Infection. Front Immunol. 2019; 10:144. Epub 2019/02/23. https://doi.org/10.3389/fimmu.2019.00144 PMID: 30787929; PubMed Central PMCID: PMC6373783.

31. Chaipan C, Soilleux Elizabeth J, Simpson P, Hofmann H, Gramberg T, Marzi A, et al. DC-SIGN and CLEC-2 Mediate Human Immunodeficiency Virus Type 1 Capture by Platelets. J Virol. 2006; 80 (18):8951–60. https://doi.org/10.1128/JVI.00136-06 PMID: 16940507

32. Nabi-Afjadi M, Heydari M, Zalpoor H, Arman I, Sadoughi A, Sahami P, Aghazadeh S. Lectins and lectibodies: potential promising antiviral agents. Cell Mol Biol Lett. 2022; 27(1):37. Epub 2022/05/14. https://doi.org/10.1186/s11658-022-00338-4 PMID: 35562647; PubMed Central PMCID: PMC9100318.

33. Julg B, Barouch D. Broadly neutralizing antibodies for HIV-1 prevention and therapy. Semin Immunol. 2021; 51:101475. Epub 20210412. https://doi.org/10.1016/j.smim.2021.101475 PMID: 33858765.

34. Sarzotti-Kelsoe M, Bailer RT, Turk E, Lin CL, Bilska M, Greene KM, et al. Optimization and validation of the TZM-bl assay for standardized assessments of neutralizing antibodies against HIV-1. J Immunol Methods. 2014; 409:131–46. Epub 20131201. https://doi.org/10.1016/j.jim.2013.11.022 PMID: 24291345; PubMed Central PMCID: PMC4040342.

35. Etchison JR, Holland JJ. Carbohydrate composition of the membrane glycoprotein of vesicular stomatitis virus grown in four mammalian cell lines. Proc Natl Acad Sci U S A. 1974; 71(10):4011–4. https://doi.org/10.1073/pnas.71.10.4011 PMID: 4372602; PubMed Central PMCID: PMC434317.

36. Dimitrov DS. Virus entry: molecular mechanisms and biomedical applications. Nature Reviews Microbiology. 2004; 2(2):109–22. https://doi.org/10.1038/nrmicro817 PMID: 15043007

37. Karsten CB, Buettner FF, Cajic S, Nehlmeier I, Neumann B, Klippert A, et al. Exclusive Decoration of Simian Immunodeficiency Virus Env with High-Mannose Type N-Glycans Is Not Compatible with

Mucosal Transmission in Rhesus Macaques. J Virol. 2015; 89(22):11727–33. Epub 2015/09/12. https://doi.org/10.1128/JVI.01358-15 PMID: 26355090; PubMed Central PMCID: PMC4645679.

38. Boyd MR, Gustafson KR, McMahon JB, Shoemaker RH, O'Keefe BR, Mori T, et al. Discovery of cyanovirin-N, a novel human immunodeficiency virus-inactivating protein that binds viral surface envelope glycoprotein gp120: potential applications to microbicide development. Antimicrob Agents Chemother. 1997; 41(7):1521–30. https://doi.org/10.1128/AAC.41.7.1521 PMID: 9210678; PubMed Central PMCID: PMC163952.

39. Balzarini J, Schols D, Neyts J, Van Damme E, Peumans W, De Clercq E. Alpha-(1–3)- and alpha-(1–6)-D-mannose-specific plant lectins are markedly inhibitory to human immunodeficiency virus and cytomegalovirus infections in vitro. Antimicrob Agents Chemother. 1991; 35(3):410–6. https://doi.org/10.1128/AAC.35.3.410 PMID: 1645507; PubMed Central PMCID: PMC245024.

40. Bonomelli C, Doores KJ, Dunlop DC, Thaney V, Dwek RA, Burton DR, et al. The glycan shield of HIV is predominantly oligomannose independently of production system or viral clade. PLoS One. 2011; 6(8): e23521. Epub 20110816. https://doi.org/10.1371/journal.pone.0023521 PMID: 21858152; PubMed Central PMCID: PMC3156772.

41. Panico M, Bouché L, Binet D, O'Connor MJ, Rahman D, Pang PC, et al. Mapping the complete glycoproteome of virion-derived HIV-1 gp120 provides insights into broadly neutralizing antibody binding. Sci Rep. 2016; 6:32956. Epub 20160908. https://doi.org/10.1038/srep32956 PMID: 27604319; PubMed Central PMCID: PMC5015092.

42. Parrish NF, Gao F, Li H, Giorgi EE, Barbian HJ, Parrish EH, et al. Phenotypic properties of transmitted founder HIV-1. Proc Natl Acad Sci U S A. 2013; 110(17):6626–33. Epub 20130329. https://doi.org/10.1073/pnas.1304288110 PMID: 23542380; PubMed Central PMCID: PMC3637789.

43. DiNapoli SR, Hirsch VM, Brenchley JM. Macrophages in Progressive Human Immunodeficiency Virus/Simian Immunodeficiency Virus Infections. J Virol. 2016; 90(17):7596–606. https://doi.org/10.1128/JVI.00672-16 PMID: 27307568

44. Spillings BL, Day CJ, Garcia-Minambres A, Aggarwal A, Condon ND, Haselhorst T, et al. Host glycocalyx captures HIV proximal to the cell surface via oligomannose-GlcNAc glycan-glycan interactions to support viral entry. Cell Rep. 2022; 38(5):110296. https://doi.org/10.1016/j.celrep.2022.110296 PMID: 35108536.

45. Lawn SD, Roberts BD, Griffin GE, Folks TM, Butera ST. Cellular compartments of human immunodeficiency virus type 1 replication in vivo: determination by presence of virion-associated host proteins and impact of opportunistic infection. J Virol. 2000; 74(1):139–45. PMID: 10590100; PubMed Central PMCID: PMC111522.

46. Munoz O, Banga R, Perreau M. Host Molecule Incorporation into HIV Virions, Potential Influences in HIV Pathogenesis. Viruses. 2022; 14(11). Epub 20221114. https://doi.org/10.3390/v14112523 PMID: 36423132; PubMed Central PMCID: PMC9694329.

47. Hazrati A, Soudi S, Malekpour K, Mahmoudi M, Rahimi A, Hashemi SM, Varma RS. Immune cells-derived exosomes function as a double-edged sword: role in disease progression and their therapeutic applications. Biomarker Research. 2022; 10(1):30. https://doi.org/10.1186/s40364-022-00374-4 PMID: 35550636

48. Karsten CB, Buettner FFR, Cajic S, Nehlmeier I, Roshani B, Klippert A, Sauermann U, Stolte-Leeb N, Reichl U, Gerardy-Schahn R, Rapp E, Stahl-Hennig C, Pöhlmann S. Supplementary information for: Macrophage- and CD4+ T cell-derived SIV differ in glycosylation, infectivity, and neutralization sensitivity [Dataset]. Dryad. 2024. https://doi.org/10.5061/dryad.hmgqnk9rm

49. Connor RI, Chen BK, Choe S, Landau NR. Vpr is required for efficient replication of human immunodeficiency virus type-1 in mononuclear phagocytes. Virology. 1995; 206(2):935–44. https://doi.org/10.1006/viro.1995.1016 PMID: 7531918.

50. Naldini L, Blömer U, Gallay P, Ory D, Mulligan R, Gage FH, et al. In vivo gene delivery and stable transduction of nondividing cells by a lentiviral vector. Science. 1996; 272(5259):263–7. https://doi.org/10.1126/science.272.5259.263 PMID: 8602510.

51. Stahl-Hennig C, Steinman RM, Tenner-Racz K, Pope M, Stolte N, Mätz-Rensing K, et al. Rapid infection of oral mucosal-associated lymphoid tissue with simian immunodeficiency virus. Science. 1999; 285(5431):1261–5. https://doi.org/10.1126/science.285.5431.1261 PMID: 10455052.

52. O'Doherty U, Swiggard WJ, Malim MH. Human immunodeficiency virus type 1 spinoculation enhances infection through virus binding. J Virol. 2000; 74(21):10074–80. https://doi.org/10.1128/jvi.74.21.10074-10080.2000 PMID: 11024136; PubMed Central PMCID: PMC102046.

53. Edinger AL, Ahuja M, Sung T, Baxter KC, Haggarty B, Doms RW, Hoxie JA. Characterization and epitope mapping of neutralizing monoclonal antibodies produced by immunization with oligomeric simian immunodeficiency virus envelope protein. J Virol. 2000; 74(17):7922–35. https://doi.org/10.1128/jvi.74.17.7922-7935.2000 PMID: 10933700; PubMed Central PMCID: PMC112323.

54. Higgins JR, Sutjipto S, Marx PA, Pedersen NC. Shared antigenic epitopes of the major core proteins of human and simian immunodeficiency virus isolates. J Med Primatol. 1992; 21(5):265–9. PMID: 1383547.

55. Schneider CA, Rasband WS, Eliceiri KW. NIH Image to ImageJ: 25 years of image analysis. Nat Methods. 2012; 9(7):671–5. https://doi.org/10.1038/nmeth.2089 PMID: 22930834; PubMed Central PMCID: PMC5554542.

56. Hennig R, Rapp E, Kottler R, Cajic S, Borowiak M, Reichl U. N-Glycosylation Fingerprinting of Viral Glycoproteins by xCGE-LIF. Methods Mol Biol. 2015; 1331:123–43. https://doi.org/10.1007/978-1-4939-2874-3_8 PMID: 26169738.

57. Shevchenko A, Tomas H, Havlis J, Olsen JV, Mann M. In-gel digestion for mass spectrometric characterization of proteins and proteomes. Nat Protoc. 2006; 1(6):2856–60. https://doi.org/10.1038/nprot.2006.468 PMID: 17406544.

58. Konze SA, van Diepen L, Schröder A, Olmer R, Möller H, Pich A, et al. Cleavage of E-cadherin and β-catenin by calpain affects Wnt signaling and spheroid formation in suspension cultures of human pluripotent stem cells. Mol Cell Proteomics. 2014; 13(4):990–1007. Epub 20140130. https://doi.org/10.1074/mcp.M113.033423 PMID: 24482122; PubMed Central PMCID: PMC3977196.

59. Cox J, Mann M. MaxQuant enables high peptide identification rates, individualized p.p.b.-range mass accuracies and proteome-wide protein quantification. Nat Biotechnol. 2008; 26(12):1367–72. Epub 20081130. https://doi.org/10.1038/nbt.1511 PMID: 19029910.

60. Cox J, Neuhauser N, Michalski A, Scheltema RA, Olsen JV, Mann M. Andromeda: a peptide search engine integrated into the MaxQuant environment. J Proteome Res. 2011; 10(4):1794–805. Epub 20110222. https://doi.org/10.1021/pr101065j PMID: 21254760.

61. Tsuchiya S, Aoki NP, Shinmachi D, Matsubara M, Yamada I, Aoki-Kinoshita KF, Narimatsu H. Implementation of GlycanBuilder to draw a wide variety of ambiguous glycans. Carbohydr Res. 2017; 445:104–16. Epub 20170419. https://doi.org/10.1016/j.carres.2017.04.015 PMID: 28525772.